J. Materials, Conc. Struct. Pavements, JSCE, No. 739/V-60, 285-296, 2003 August

FUNDEMENTAL PURE TORSIONAL PROPERTIES OF CONCRETE FILLED CIRCULAR STEEL TUBES

Jehyun BECK[1] and Osamu KIYOMIYA[2]

[1]Member of JSCE, Dr. Eng., Research Associate, Dept. of Civil Eng., Waseda University
(16F-01, 3-4-1 Okubo Shinjuku-ku, Tokyo 169-8555, Japan)
E-mail:beck@aoni.waseda.jp
[2]Fellow of JSCE, Dr. Eng., Professor, Dept. of Civil Eng., Waseda University
(16F-01, 3-4-1 Okubo Shinjuku-ku, Tokyo 169-8555, Japan)
E-mail:k9036@waseda.jp

Static loading tests on steel columns and composite columns were carried out in order to investigate basic properties of torsion. Moreover, the results of loading test were compared with theoretical analysis and F.E.M. (Finite Element Method) analysis, considering nonlinear material properties. From the comparative works, following conclusions were obtained. At the test, the failure of steel columns was determined by local buckling. Composite columns had much higher bearing capacity than steel columns because local buckling of steel column was prevented by filled concrete. Torsional moment on yield point and torsional rigidity in the theoretical analysis and the results of F.E.M. analysis had almost corresponded to those of loading tests.

Key Words : *torsion, composite column, local buckling, torsional rigidity, F.E.M. analysis*

1. INTRODUCTION

The structural design for many structures is performed so that a large torsional moment may not occur, and the considering of torsion is usually abbreviated. However, there are cases that torsional moment cannot be ignored for large-sized unsymmetrical structures or the direction of eccentric load action. For examples, when the horizontal force due to earthquake acts on a building or a substructure of a bridge which has unsymmetrical configuration, a large torsional moment may occur at columns and slabs. Moreover, it is also important for the problem of torsion such as the large-sized gravity type structures which receive non-uniformed subsidence of soft ground, the floating type structures which receive wave force from slant direction and the pile type structures which receive eccentric load by an earthquake or loading of a vessel in recent years[1)]. Composite members which consist of steel and concrete have been applied such structures in these a couple of decades. Composite members have been applied to various kinds of structures, such as a bridge, offshore structures and so on because composite members have high strength characteristics and deformation capacity.

Many researches have been conducted on steel members and reinforced concrete members. The mechanical properties and characteristics have been considerably grasped by experimental studies etc. The design formulas have also been proposed. However, the mechanical properties of composite members subjected to torsion are not well known in contrast to composite members subjected to bending, shear and axial force. The considered examples on torsion are also limited for the composite members. There are also few proposals for design formulas, and it is hard to say that those are enough checked about applicability. Composite members with steel column and core concrete is studied in this paper.

Thus, static loading tests of pure torsion were carried out in order to investigate basic properties of torsion and mechanical behavior. The loading tests are performed on a concrete column, steel columns and composite columns with circular cross section

Table 1 List of test specimens and their main dimensions

Tests	Specimen	Classification	Thickness of steel	D/t
Test series 1	CC	Concrete column	——	—
	CS35	Steel column	3.5mm	39.9
	CS45		4.5mm	31.1
	CH35	Composite column	3.5mm	39.9
	CH45		4.5mm	31.1
Test series 2	CS40	Steel column	4.0mm	35.0
	CH40	Composite column		
	CH40-BS			

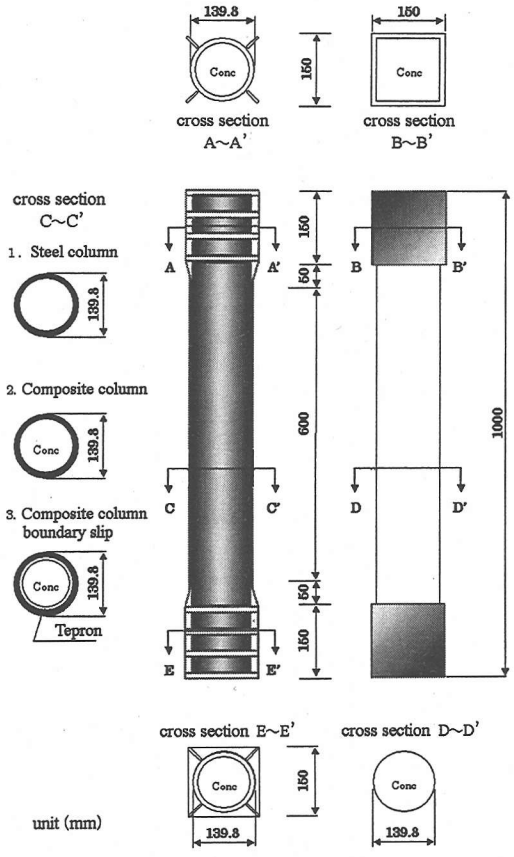

Fig. 1 Dimensions and basic structure of the specimens

on condition that one end is fixed and the other end is applied by torsion. In addition, finite element method analysis, considering the nonlinear material properties by the SOLVIA program was performed, and comparison with the results of experiments and theoretical analysis was carried out.

2. EXPERIMENTS

(1) Specimens

The list of test specimens and their dimensions are presented in **Table 1**. The dimensions and outline of the specimens are shown in **Fig. 1**. Diameter / thickness (D/t) is ranged from 31.1 to 39.9 in the specimen. The loading tests were divided into two test groups. Two specimens of steel columns and two specimens of composite columns in the thickness of steel plates of 3.5mm and 4.5mm were used for the test series 1. And one specimen of concrete column was also used for the test series 1. At the test series 2, one steel column and two composite columns of 4.0mm thick steel plate of different boundary conditions were used to investigate the adhesion and the behavior of filled concrete at the boundary between steel plate and concrete. One of them was constructed as same as test series 1 which was assumed that steel and concrete are firmly bonded. The other one had the tepron sheet, which was installed into the boundary between steel plate and concrete to make filled concrete slip at the boundary. Molds were made of mortar and installed as shown in **Photo 1** for measuring strains at surface on the filled concretes

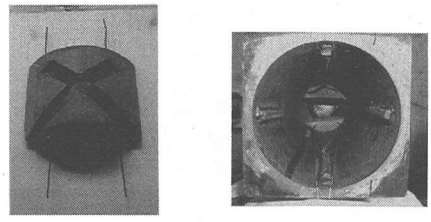

Photo 1 Strain measurement at surface on filled concrete in case of CH40 and CH40-BS specimen

Table 2 Specified mix proportion of the concrete

Max. size of coarse aggregate (mm)	Water-cement ratio (%)	Sand-aggregate ratio (%)	Unit contents (kg/m^3)				
			Water	Cement	Fine aggregate	Coarse aggregate	Admixtures
25	50.3	43.8	164	326	780	1012	3.52

Table 3 Material properties of the concretes

Specimens	Strength (MPa)		Young's Modulus Ec (MPa)	Poisson's Ratio ν
	Compressive	Tensile		
Concrete column CC	31.7	2.86	2.03×10^4	0.133
Composite column CH35	31.2	2.71	2.86×10^4	0.205
Composite column CH40	27.0	2.60	2.27×10^4	0.180
Composite column CH45	33.0	2.83	2.86×10^4	0.188

Table 4 Material properties of steel plates

Thickness of test pieces	Yielding Stress (MPa)	Tensile Strength (MPa)	Young's Modulus Es (MPa)	Poisson's Ratio ν
3.5mm	322.9	459.6	2.1×10^5	0.26
4.0mm	340.3	417.0	2.3×10^5	0.28
4.5mm	348.2	426.8	2.1×10^5	0.28

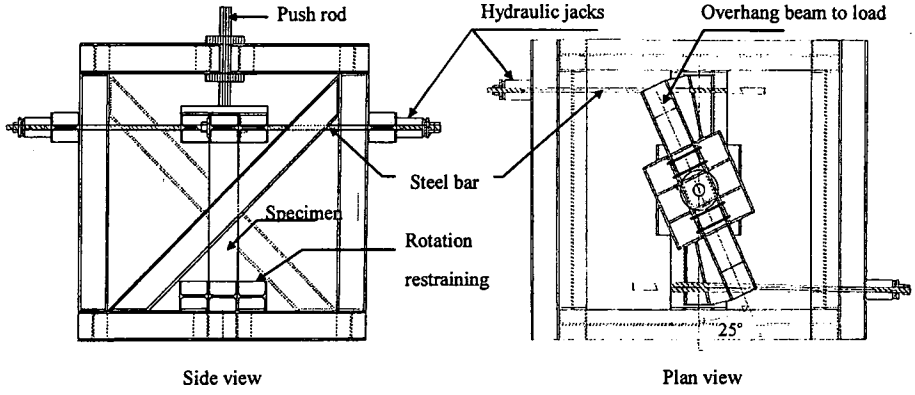

Fig. 2 Test set-up

at this test series 2. The height of the specimen was 1m and its outer diameter of cross section was 139.8mm by any specimen. Reinforcement of end boxes for each specimen was performed using inside concrete arranged in the range of 150mm from both ends.

(2) Materials

Table 2 shows the specified mix proportion of concrete used for the specimens. The basic strength for the design of concrete was 30MPa. The slump and the air content of concrete were 10cm and 4.0%, respectively. Concrete using ordinary Portland cement was casted inside into steel column. **Table 3** indicates the material properties of concrete at the age of the loading test. These values were obtained from the tests with the control cylindrical specimens which size was Ø10 × 20cm. The STK41 of steel plate was used for the specimens. Assured tensile strength of steel plate was 400MPa. The results of tensile tests carried out on the test pieces are shown in **Table 4.**

(3) Test procedures

Fig. 2 shows the loading set-up. A pure torsional moment was applied through the overhang beam from upper bearing pressure plate to the top end of a specimen. To produce the required torsion, two hydraulic jacks were installed to apply reversal tensile forces. Supporting point of bottom end was fixed and the other end was free for torsion. The monotonous load was applied statically, taking care of that the amount of drawing in of two hydraulic jacks becomes almost equal at each loading step.

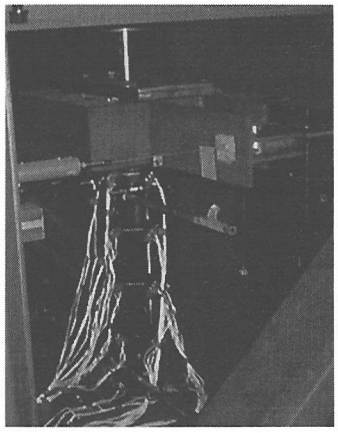

Photo. 2 General view of test set-up

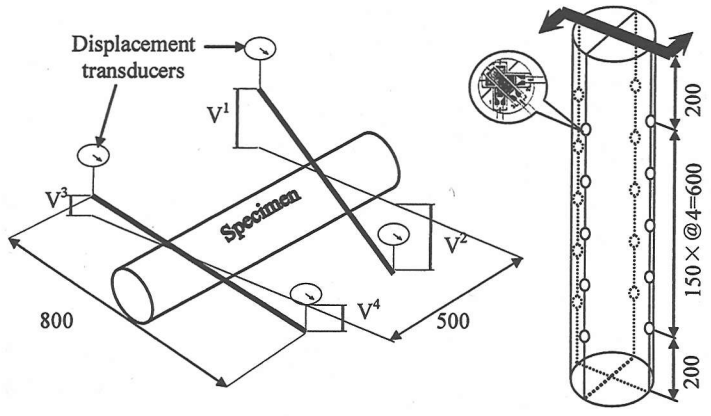

Fig. 3 Arrangement of displacement transducers and strain gauges

(4) Measurement procedure

Photo. 2 shows the general view of test set-up. The applied load was measured using load cells installed on the jacks. Movement of the jack axis was measured by displacement transducers. **Fig. 3** shows the positions of rotation angle measurements and deployment of strain gauges on the specimen. Aluminum bars were arranged in the 250mm place from the both ends of specimen. Each rotation angle was measured from the difference between the displacement of V1 and V2, and the difference between the displacement of V3 and V4. The angle of twist was determined by the change of the rotation angle per unit length from the differences of these rotation angles[2].

3. EXPERIMENTAL RESULTS

(1) Torsional rigidity

According to the typical relationship between torsional moment T and angle of twist per unit length θ, following equation is presented[3],

$$T = G J \theta \quad (1)$$

in which G is the shear modulus of elasticity and J is known in general as the torsion constant. The quantity GJ, called the torsional rigidity and indicate the tangency of torque-rotation curve, was used for the comparison with each test results as presented in **Table 5**.

(2) Steel column

Torque-rotation curves of three steel columns obtained from the loading tests are plotted in **Fig. 4**. The general behaviours in steel column were such that, initially linear elastic response in a low loading stage was observed. The load gradually increased up to Ty where the torque-rotaition curve is bent(rounded) exhibiting non-linear response from yielding of the steel tubes. Torsional rigidity in the loading test also began to show non-linear properties by approaching yield point according to high load value. The ductility μ of each specimen under pure torsion was determined using angle of twist θ from

Table 5 Comparison with each specimen with 4.5mm thick steel plate

	Concrete column A	Steel column B	Simple accumulation C = A + B	Composite column D	Ratio (D/C)
Ty (kN·m)	1.19	26.4	27.6	31.9	1.16
$Tmax$ (kN·m)	1.19	30.6	31.8	40.1	1.26
GJ (kN·m²)	306	648	954	903	0.95
Ductility μ	——	8.6	——	Over 10	——

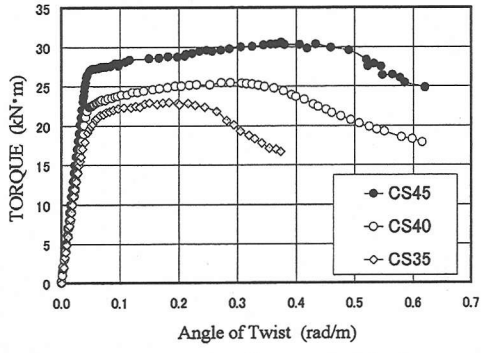

Fig. 4 Torque-rotation diagram of steel columns

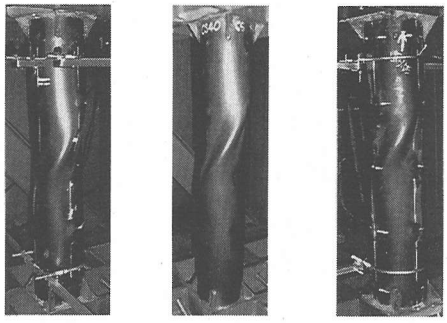

CS35 CS40 CS45

Photo. 3 Local buckling of steel specimens

the yield point. it had the ductility of 8 times or more after the yield of steel columns. It seems that more gain in ductility was obtained for steel columns with larger thickness.

Finally, buckling was initiated at the peak load ***Tmax***, the load carrying capacity reduced with increasing angle of twist. The failure of steel columns was determined by local buckling as shown in **Photo 3**. The buckling was not fully symmetric, which leaded to some load eccentricity. Local buckling were concentrated at the middle of the tube in general. The bearing capacity in the experiments decreased under the influence of local buckling.

(3) Concrete column

The Torque-rotation curve of concrete column obtained from the loading test are shown in **Fig. 5**. It appears that rapid collapse occurred after reaching peak load. Unlike the steel column, failure was occurred in the upper part of the column.

(4) Composite column

Torque-rotation curves of three composite columns obtained from the loading tests are plotted in **Fig. 6**. In composite column, the slope of the torque-rotation curve shows initially linear elastic response up to about 20% of the yield torsional moment where the torque-rotation curve is bent(rounded) exhibiting non-linear response from yielding of the composite column. However, after the crack occured in concrete, the torsional rigidity of specimen decreased and it became the torsional rigidity of only the steel plate. Once a penetrating crack occurs inside of the column, it could be said that torsional rigidity cannot be accumulated to that of steel column. Torsional bearing capacity on the loading tests did not fall where the angle of twist even reaches 10 times or more than the point where the torque-rotation curve is bent. As shown in **Fig. 6** the applied torque moment tended to increase even at the end of the loading. In these cases, the ultimate torsional moment was defined as the one at which the angle of twist reached 20 degrees due to the restriction in the test equipment. The ultimate torsional moment in composite column was 1.26 times higher than the value that simply accumulated from the bearing capacities of concrete and steel column in the loading tests separately. Torsional bearing capacity of composite column was maintained high after steel yield. Remarkable large deformation capacity was obtained, and local buckling has been prevented by filled concrete. This result indicates that the torsional bearing capacity in composite column became high by filling concrete into steel column, and it was acquired that composite column had the remarkable synthetic effect.

In general, the performance of the composite section under the torsion is better than the steel column, particularly in the post-peak response. It can be seen that the composite columns with the angle of twist are more ductile, where the post peak curve is flat compared to those for the steel columns.

The steel plate of composite column was removed after the loading test, and the crack pattern of the filled concrete was shown in **Photo 4**. The cracks were observed on the whole surface with regular intervals, and the direction of the cracks was almost 45 degrees. It is evident that the shear failure was occurred at the filled concrete in composite column.

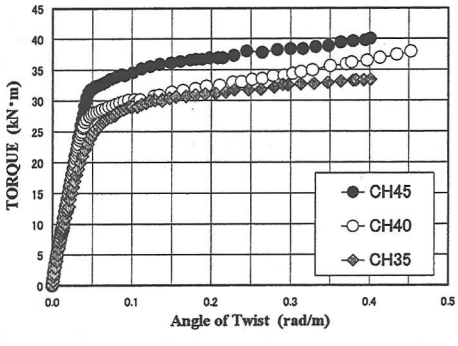

Fig. 5 Torque-rotation diagram of concrete column

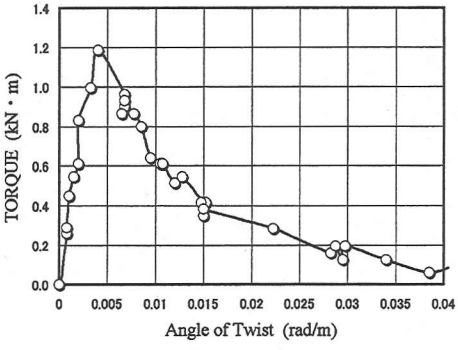

Fig. 6 Torque-rotation diagram of composite columns

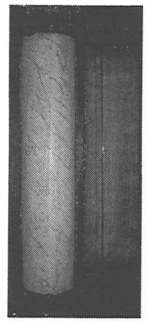

Photo. 4 Cracks on fiiled concrete

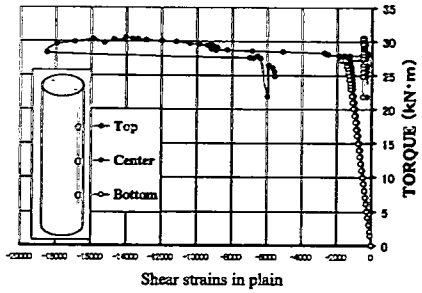

Fig. 7 Torque-strain curves in CS45 specimen

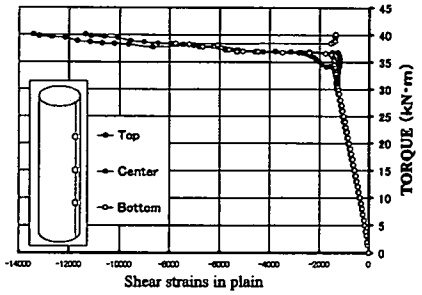

Fig. 8 Torque-strain curves in CH45 specimen

(5) Strains on the steel plate

Torque-strain curves in CS45 specimen and CH45 specimen in case of 4.5mm thick steel plate are shown in **Fig. 7** and **Fig. 8**. Shear strains in plain which were calculated from three measured axial strains are plotted in both torque- strain curves. Shear strains in plain had the high value in the both steel and composite column. Strains on center and bottom end made a reverse turn after yield in the steel column as shown in **Fig. 7**. This phenomenon is due to the buckling of the steel. However, those on composite column kept increasing and did not fall down until the applied loading was removed.

(6) The behaviour of filled concrete

Molds were installed into two composite columns of 4.0mm thick steel plate which have different boundary conditions in order to investigate the behavior of filled concrete. One of them is CH40 specimen which was assumed that steel and concrete are firmly bonded. The other one is CH40-BS specimen which had the tepron sheet to make filled concrete slip at the boundary. The observed strains from both left and right side on the surface of filled concrete of each specimens are shown in **Fig. 9** and **Fig. 10**. Torque-rotation curves of three specimen which have same steel plate of 4.0mm thick are also plotted in **Fig. 11**.

In CH40 specimen, the strains of filled concrete after cracks occurred were continued increasing until steel plate yielded. However, those of CH40-BS specimen after cracks occurred were diffused, and the torsional bearing capacity was lower than CH40 specimen. Torsional yield moment *Ty* of CH40-BS specimen has the very similar result to the value which simply and separately accumulated from concrete column CC and steel column CS40 obtained from the loading tests as presented in **Table 6**.

Table 6 Comparison with specimen which steel plate is 4.0mm thick

	CC A	CS B	Accumulation C = A + B	CH40-BS D	CH40 E	Ratio (D/C)	Ratio (E/C)	Ratio (E/D)
Ty (kN·m)	1.19	22.0	23.2	23.5	27.5	1.01	1.19	1.17
Tmax (kN·m)	1.19	25.4	26.6	36.7	42.0	1.34	1.58	1.14
GJ (kN·m²)	306	513	819	877	882	1.07	1.08	1.01
Ductility μ	——	8.6	——	Over 13.72	Over 12.32	——	——	——

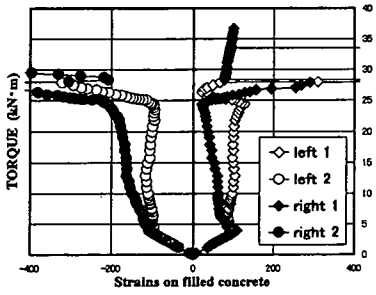

Fig. 9 Torque-strain curves of molds in CH40-BS specimen

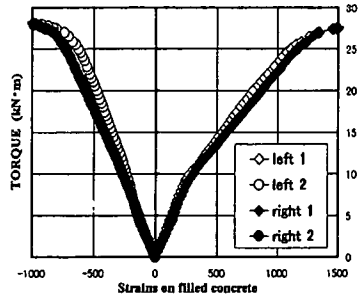

Fig. 10 Torque-strain curves of molds in CH40 specimen

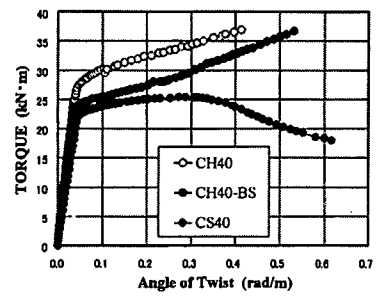

Fig. 11 Torque-rotation curves of each specimen with 4.0mm steel plate

However, ultimate torsional moment ***Tmax*** of CH40-BS had 1.34 times high value than that of accumulated result because the buckling of steel plate was prevented by filled concrete. The torsional rigiditiy did not have large differncy from both composite column and accumulated result. It was obvious no matter how both bearing capacities are different between CH40 and CH40-BS, the torsional rigidities were almost equal as shown in **Fig. 11** and **Table 6**. Therefore, the torsional rigidity in composite column becomes that of only the steel plate after the crack occured in filled concrete as discussed in previous studies[4),5)].

The behaviour of filled concrete in case of firmly bonded composite column was such that the remarkable synthetic effect was acquired according to the bearing capacity increased until steel plate yields even if the cracks were occurred in filled concrete.

4. THEORETICAL ANALYSIS

(1) Torsional moment

a) Solid circular bar for concrete column

According to the Mechanics of Materials[3)], the maximum shear stress τ_{MAX} and the torsional moment Tc in this bar are presented as,

$$\tau_{MAX} = Tc\ r / Ip \tag{2}$$

This equation, known as the torsion formula, shows that the maximum shear stress is proportional to the applied torque Tc and radius r, and inversely proportional to the polar moment of inertia Ip of the cross section. Substituting $r = d/2$ and $Ip = \pi d^4/32$, next equation derived.

$$Tc = \frac{\pi d^3}{16}\ \tau_{MAX} \tag{3}$$

as the formula for the torsional moment in a solid circular bar. In concrete column, the maximum shear stress τ_{MAX} is represented to tensile strength of concrete σ_t.

b) Thin-walled tube for steel column

The product of the shear stress τ and the thickness t of this thin-walled tube is the same at every point in the cross section. This product is known as the shear flow f.

$$f = \tau t = \textbf{constant} \tag{4}$$

The torsional moment Ts produced by the shear stresses is obtained by integrating along the entire length of the median line of the cross section.

$$Ts = 2fAm \tag{5}$$

where Am is the area enclosed by the median line of the cross section. From this equation, we get

$$Ts = 2Amt\ \tau \tag{6}$$

c) Composite column

Torsional moment T_H in composite column is assumed that the composite bar is acted upon by a total torque, which is resisted by torque Tc^* and Ts in the solid circular bar and thin-walled tube, and expressed as,

$$T_H = Tc^* + Ts \tag{7}$$

in which, Tc^* is fully plastic torsional moment obtained from Sand Hill Analogy[6),7)], and presented as,

$$Tc^* = \frac{\pi d^3}{16}\ \tau_C^* \tag{8}$$

where τ_C^* is shear strength of filled concrete,

According to the modified Mohr-Coulomb failure criterion in reinforced concrete diaphragm subjected to shear, the average shear strength τ_C^* and compressive strength f_C are presented as[8)],

$$\frac{\tau_C^*}{f_C} = \frac{1-\sin\alpha}{2\cos\alpha} + \psi\tan\alpha \tag{9}$$

where, α : angle between the yield line and loading direction

ψ: degree of reinforcement

From the upper-bound solutions, the angle α and ψ are the positive value determined by strength of steel and concrete. If there were high restrains, such as steel pipe restrains concrete behavior in composite column, α can be assumed to be zero and next equation would be presented.

$$\tau_C^* = \frac{f_C}{2} \tag{10}$$

Thus, shear strength of filled concrete becomes large because it restrains that the width of crack generated by shear becomes wide with an outside steel plate.

(2) Torsion constant and torsional rigidity

It has mentioned that the typical relationship between torsional moment T and angle of twist per unit length θ is presented in **Eq(1)**.

a) Solid circular bar for concrete column

In case of concrete column, torsional constant J_C is presented as,

$$Jc = \frac{\pi d^4}{32} \tag{11}$$

Table 7 Comparison of torsional rigidity between theoretical analysis and test result in case of CH40 specimen

Theory			Test		Ratio	
Concrete A	Steel B	Accumulated C	Initial D	After crack E	Step 1 (C/D)	Step 2 (B/E)
$G_C J_C$	$G_S J_S$	$G_C J_C + G_S J_S$	GJ	GJ		
291	642	933	882	639	1.06	1.00

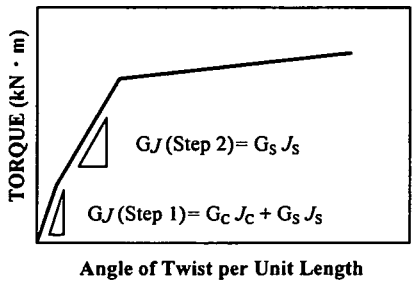

Fig. 12 Outline of torsional rigidy in composite column

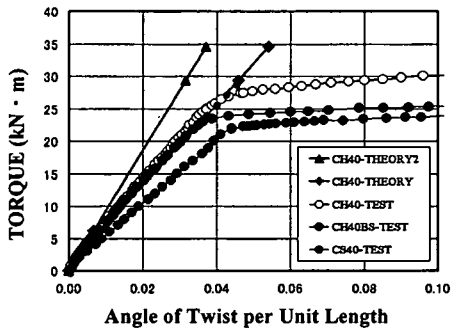

Fig. 13 Comparison of torsional rigidity between theoretical analysis and test result

this torsional constant J_C agrees with polar moment of inertia Ip in the solid circular bar for concrete column.

b) Thin-walled tube for steel column

In case of steel column, torsional constant J_S is presented as,

$$Js = \frac{4\,t\,A_m^2}{L_m} = \frac{\pi d^3}{4} \qquad (12)$$

where L_m is the length of the median line of the cross section. The polar moment of inertia Ip is also approximately agrees with torsional constant J_S in the thin-walled tube.

c) Torsional rigidity for composite column

Following equation is obtained from the premise that the angle of twist per unit length θ are the same for both steel column and filled concrete column because they are firmly bonded together[3].

$$T = G\,J\,\theta = Tc + Ts = (G_C J_C + G_S J_S)\,\theta \qquad (13)$$

However, there was a tendency that torsional rigidity GJ falls at the stage where a torsional moment is comparatively small. It has been grasped in the previous studies and experiments[4),5)] that once penetrating crack occurs inside of the filled concrete, the torsional rigidity of composite column decreased. Therefore, contribution of the concrete for torsional rigidity is very small. It could be said that torsional rigidity of concrete cannot be accumulated to that of steel column after the crack occured in filled concrete in design when D/t is about 40.

Hence, torsional rigidity of composite column in this paper was analyzed into two steps. One is before the penetrating crack arises and, the other is after arisen as shown in **Fig. 12**. At the first step, the torsional rigidity of composite column is calculated by accumulating both torsional rigidity of steel and filled concrete. After the value of the failure torsional moment of filled concrete, it becomes the torsional rigidity of only the steel plate. **Table 7** presents the comparison of torsional rigidity between theoretical analysis and test result in case of CH40 specimen in detail. **Fig. 13** also shows the result of comparison. It was made reference that the result, which carried out simple accumulation on the whole members, was also shown as CH40-THEORY2. It is much higher than both CH40-THEORY(theoretical analysis) and CH40-TEST in contrast to CH40 -THEORY has almost equal to the test result after crack occurred (analysis in step 2). From these results, it has known that the accumulating method in two steps brings good agreement with test result.

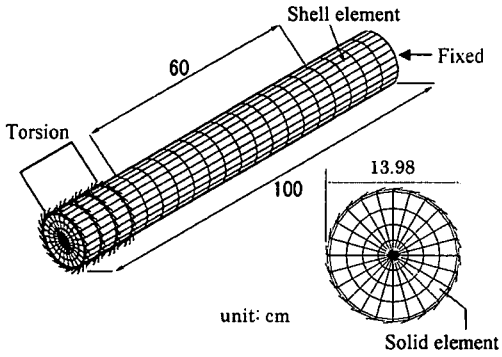

Fig. 14. Finite element model

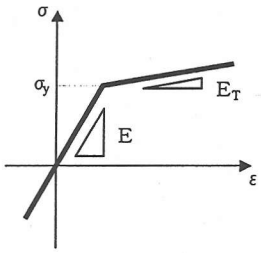

Where, σ_y : Yield stress
E : Young's modulus
$\mathbf{E_T}$: Strain hardening modulus

Fig. 15 Bilinear stress-strain relationship for steel

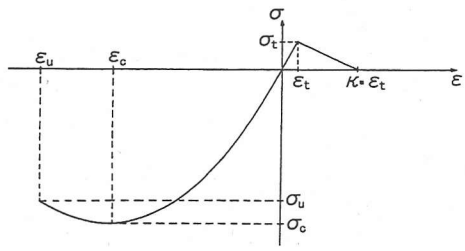

Where, σ_t : Cut-off tensile stress
σ_u : Ultimate compressive stress
σ_c : Maximum compressive stress

Fig.16 Uniaxial stress-strain curve for concrete

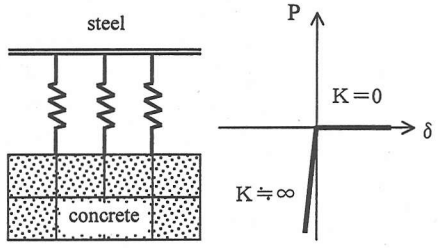

Fig. 17 Spring model of normal direction

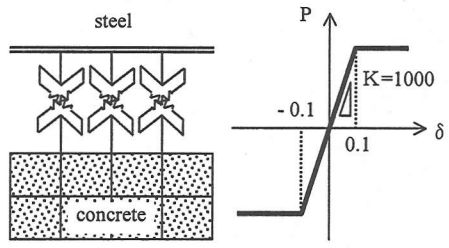

Fig. 18 Spring model of shear direction

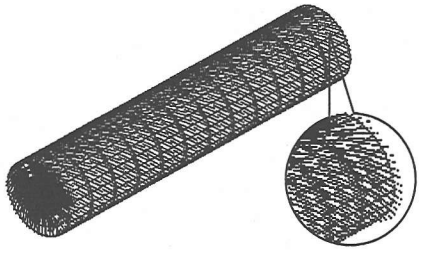

Fig. 19 Pattern of crack on filled concrete

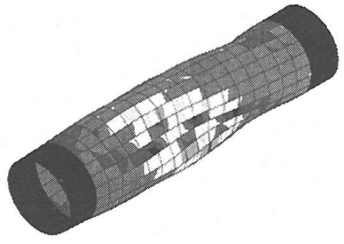

Fig. 20 Local buckling of steel column

5. FINITE ELEMENT ANALYSIS

(1) Finite element model

The SOLVIA finite element analysis program was used to analyze a concrete column, steel columns and composite columns subjected to torsion with consideration of the nonlinear material properties. **Fig. 14** shows the mesh of the finite element models in case of composite column. Because specimen used for the loading test was made into the model, the portion comparing the analysis results and test results is the range of 60cm shown in **Fig. 14.** Cylindrical 4-node thin shell elements and the 8-node solid elements were used in the modeling of the steel tube and concrete column, respectively.

(2) Material model

The bilinear type nonlinear material model was used in steel column as a material model as shown in **Fig. 15**. Strain hardening modulus $\mathbf{E_T}$ is assumed to be 1/100 of young's modulus **E**. The concrete model of uniaxial stress / strain relationship is shown in **Fig. 16**. It was used for concrete column. When a tensile failure has occurred, the stress normal to the tensile failure plane decreases linearly with the strain to a zero value. Kappa in the figure shows a coefficient of maximum tensile strain to the strain at initial crack. Value of kappa of 150 is adopted here according to past researches and problem of convergence during iteration calculation. The values of σ_t, σ_u, σ_c, ε_c and ε_u are determined by loading tests for cylindrical concrete specimen of ϕ 100mm. This model does not estimate crack width and crack region is presented by smeared region. Uniform distribution load was applied to the range of 20cm of the free end to produce the required torsion to the steel column of finite element model.

(3) Spring Model

In order to take a slip and mutual friction into consideration at the boundary between steel plate and filled concrete in the composite column, the spring element that expresses an adhesion was used at the normal direction and shear direction. **Fig. 17** and **Fig. 18** show elements and material models of the spring in each direction. For normal direction, spring constant is zero for tension side and fairly large value for compression side. For shear direction, by-linear relationship is adopted and yield point is obtained by maximum friction between the steel and concrete. A Mohr-coulomb yield criterion of the concrete is applied for determination of maximum friction. When tepron sheet is used to decrease the friction, the friction coefficient of 0.1 is used.

(4) Analysis Result

As a result of the F.E.M (Finite Element Method) analysis, pattern of crack on filled concrete and local buckling on steel column in case of the composite column of thickness 4.5mm at the final step is shown in **Fig. 19** and **Fig. 20** respectively. If a tube subjected to torsion has very thin walls, the possibility that the walls will buckle must be taken into account. And it was found that torsional bearing capacity declined remarkably because the failure of these steel columns was determined by local buckling at the experiments. Therefore, abrupt reduction in the strain hardening modulus E_T after reaching a yielding point was considered for the analysis of buckling on the steel column. Applying lateral force or compulsory displacements to induce the buckle were not considered in this buckling analysis.

6. COMPARISON

(1) Concrete column

The relationships between torsional moment and angle of twist about each result obtained from the theoretical analysis, F.E.M. analysis and the loading test are shown in **Fig. 21**. The results of theoretical analysis and F.E.M. analysis are also compared with test results in **Table 8**. It could be observed from **Table 8** that the F.E.M. analysis agrees very well with the test results on the both failure torsional moment and torsional rigidity. The theoretical prediction on the failure torsional moment of 1.34 kN·m was 1.13 times higher than the test result of 1.19 kN·m, but almost same result with the test result was obtained on torsional rigidity.

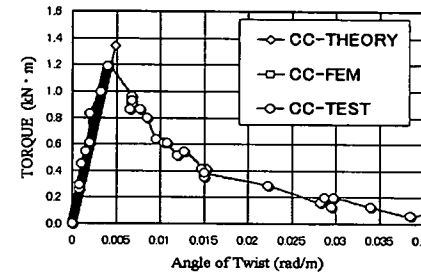

Fig. 21 Each result in CC specimen

Table 8 Comparison in concrete column

	Theory A	F.E.M. B	Experiment C	Ratio (A/C)	Ratio (B/C)
Torsional moment (kN·m)	1.34	1.19	1.19	1.13	1.00
Torsional rigidity (kN·m^2)	274	295	306	0.89	0.96

Table 9 Comparison in steel column

	Specimen	Theory A	F.E.M. B	Experiment C	Ratio (A/C)	Ratio (B/C)
Yield torsional moment (kN·m)	CS35	19.4	18.8	19.9	0.98	0.94
	CS40	23.2	19.4	22.0	1.05	0.88
	CS45	26.5	25.8	26.4	1.00	0.98
Ultimate torsional moment (kN·m)	CS35	27.6	19.7	23.0	1.20	0.86
	CS40	28.4	23.1	25.4	1.12	0.91
	CS45	32.3	30.7	30.6	1.06	1.00
Torsional rigidity (kN·m^2)	CS35	577	556	504	1.14	1.10
	CS40	641	616	513	1.25	1.20
	CS45	717	700	648	1.11	1.08

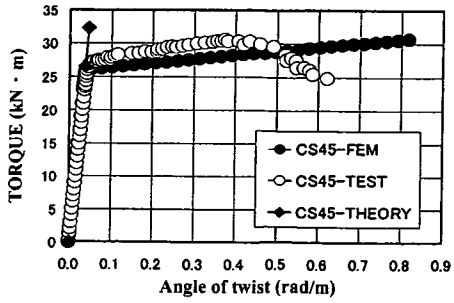

Fig. 22 Each result in CS45 specimen

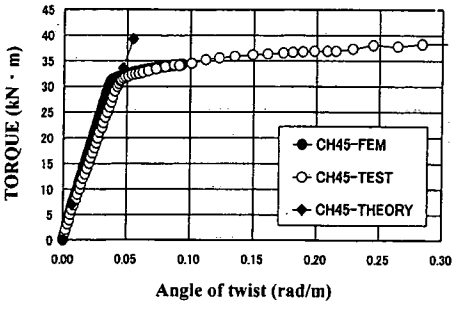

Fig. 23 Each result in CH45 specimen

(2) Steel column

A comparison is made with the theoretical analysis, F.E.M. analysis and the loading test in **Table 9**. In case of 4.5mm thick steel column, torque-rotation curves of each result in the comparison are plotted in **Fig. 22**. Torsional rigidity of test result was about 10 to 20% smaller than theoretical analysis and F.E.M analysis as presented in **Table 9**. Torsional yield moment of test value brought the results, which is almost equal to those of theoretical analysis and F.E.M. analysis. However, ultimate torsional moment of the theoretical analysis became higher than experiments on the whole, this is because the bearing capacity in the experiments decreased under the influence of local buckling. On the other hand, ultimate torsional moment of F.E.M. analysis had the lower value than experiments. It was caused by abrupt reduction in the strain hardening modulus E_T after reaching a yielding point for considering in local buckling. It had also high value when local buckling did not considered in the F.E.M. analysis.

(3) Composite column

Table 10 lists the compared results obtained from the theoretical analysis, F.E.M. analysis and the loading test. **Fig. 23** also compares the torque -rotation curves obtained from those results in case of 4.5mm thick composite column. A good agreement was obtained between F.E.M. analysis and experiment for initial torsional rigidity. However, the increase of angle of twist was smaller than loading test after cracks occurred in filled concrete. Torsional rigidities, which were compared in **Table 10** between theoretical analysis and experiment, were dealed with initial values and those differencies were large a little. Torsional rigidities of theoretical analysis have almost equal to the test result after cracks occurred in filled concrete (analysis in step 2) as mentioned in 4-(2)-c). The theoretical analysis and F.E.M. analysis brought the similar results with experiment for yield torsional moment as presented in **Table 10**. The ultimate torsional Moment on the loading test was about 10 to 20% as high as that of theoretical analysis and F.E.M analysis because of high ductility. Remarkable synthetic effect was acquired in composite columns because the bearing capacity increased until steel plate yields even if the cracks were occurred in filled concrete. Contrary to steel columns, local buckling did not occur in composite column.

Table 10 Comparison in composite column

	Specimen	Theory A	F.E.M. B	Experiment C	Ratio (A/C)	Ratio (B/C)
Yield torsional moment (kN·m)	CH35	27.2	23.7	26.7	1.02	0.89
	CH40	29.4	26.2	27.5	1.07	0.95
	CH45	33.5	31.8	31.9	1.05	1.00
Ultimate torsional moment (kN·m)	CH35	35.4	27.0	33.4	1.06	0.81
	CH40	34.6	32.7	42.0	0.82	0.78
	CH45	39.3	34.3	40.1	0.98	0.85
Torsional rigidity ($kN·m^2$)	CH35	940	858	842	1.12	1.02
	CH40	933	906	882	1.06	1.03
	CH45	1006	979	903	1.18	1.08

7. CONCLUSIONS

The results presented in this paper are related to CFT (Concrete Filled steel Tube) subjected to pure torsion for about 30 D/t. Their behaviors under torsional load in the loading test are compared with those of theoretical analysis and F.E.M. analysis. From the result of comparative works, following conclusions are obtained.

(1) The failure of steel columns was determined by local buckling, on the other hand, torsional bearing capacity of composite column was maintained after steel yield. Remarkable large deformation capacity was obtained and concrete filling fully prevents local buckling in composite column. This result shows that the torsional bearing capacity of the composite column with filled concrete was about 20% higher than the value by simple accumulation of concrete and steel, and a remarkable synthetic effect was acquired.

(2) There was a tendency that torsional rigidity falls at the stage where a torsional moment was comparatively small. Once a crack occurred inside of the column, it would be said that the torsional rigidity of concrete could not be accumulated to that of steel.

(3) In the behavior of filled concrete, it was obvious that the torsional rigidities were almost equal among the specimens whether the boundary between steel and concrete was firmly bonded or not although those bearing capacities were different. Strain measurements indicated no slip has taken place until failure in CH40 specimen, thus perfect bond between the steel and concrete would be assumed. When tepron sheet was installed between concrete and steel, slip was observed and the strains on the surface of concrete were not coincided with the strain of steel.

(4) The theoretical analysis by accumulation design method and F.E.M. analysis considered material non-linearity of both concrete and steel were in good agreement in view of torsional rigidity and maximum bearing capacity of the composite columns from the comparative works.

REFERENCES

1) Yamada, M., Kiyomiya, O. and Yokoda, H.: Torsional properties of long caisson fabricated by hybrid members, *Transactions of the Japan Concrete Institute.*, Vol. 13, 1991
2) Mizuno, E., Shen, C. and Usami, T.: A cyclic torsion test of structural, steel member and two-surface model simulation, *Journal of Structural Engineering*, Vol. 39A, pp.221-234, 1993. (in Japanese)
3) Timoshenko, S.P. and Gere, J.M.: *Mechanics of Materials*, McGraw-Hill, 3rd edition., Newyork, pp.158-219, 1990.
4) Beck, J.H., Hirose, K. and Kiyomiya, O.: Experimental study of steel member and composite member subjected to torsion, *Journal of Constructional Steel*, Vol. 7, pp.217-224, 1999. (in Japanese)
5) Beck, J.H., Hirose, K. and Kiyomiya, O.: Static loading tests and F.E.M. analysis of steel and composite member with circular cross section subjected to torsion, *Proceedings of First International Conference on Steel & Composite Structures*, Vol. 2, pp.1319-1326, 2001.
6) Nakai, H., Kitada, T., Yoshikawa, O., Murakami, S. and Sakuramoto, Y.: Experimental study of concrete-filled steel members with circular cross section subjected to bending and torsion, *Proceedings of the JSCE*, No.612/I-46, pp.85-97, 1999. (in Japanese)
7) Izumi, M.: *Design method of concrete member subjected to torsion*, Gihoudo, pp.27-104, 1972.
8) Chen, W.F.: *Plasticity in reinforced concrete*, McGraw-Hill, pp.301-317, 1982.

(Received August 5, 2002)